The Solar and Southern Oscillation Components in the Satellite Altimetry Data

Howard, Daniel; Shaviv, Nir J.; Svensmark, Henrik

Published in:
Journal of Geophysical Research: Space Physics

Link to article, DOI:
10.1002/2014JA020732

Publication date:
2015

Document Version
Publisher's PDF, also known as Version of record

AGU PUBLICATIONS

JGR

Journal of Geophysical Research: Space Physics

RESEARCH ARTICLE

10.1002/2014JA020732

Key Points:
- The Sun and ENSO explain most of the decadal sea level changes
- Solar forcing is about 8 times the changes in the irradiance

Correspondence to:
N. J. Shaviv,
shaviv@phys.huji.ac.il

Citation:
Howard, D., N. J. Shaviv, and H. Svensmark (2015), The solar and Southern Oscillation components in the satellite altimetry data, *J. Geophys. Res. Space Physics*, *120*, 3297–3306, doi:10.1002/2014JA020732.

Received 24 OCT 2014
Accepted 10 APR 2015
Accepted article online 15 APR 2015
Published online 13 MAY 2015

The solar and Southern Oscillation components in the satellite altimetry data

Daniel Howard[1], Nir J. Shaviv[2,3], and Henrik Svensmark[4]

[1]City of London School, London, UK, [2]Racah Institute of Physics, Hebrew University of Jerusalem, Jerusalem, Israel, [3]School of Natural Sciences, Institute for Advanced Study, Princeton, New Jersey, USA, [4]National Space Institute, Technical University of Denmark, Lyngby, Denmark

Abstract With satellite altimetry data accumulating over the past two decades, the mean sea level (MSL) can now be measured to unprecedented accuracy. We search for physical processes which can explain the sea level variations and find that at least 70% of the variance in the annually smoothed detrended altimetry data can be explained as the combined effect of both the solar forcing and the El Niño–Southern Oscillation (ENSO). The phase of the solar component can be used to derive the different steric and eustatic contributions. We find that the peak to peak radiative forcing associated with the solar cycle is 1.33 ± 0.34 W/m^2, contributing a 4.4 ± 0.8 mm variation. The slow eustatic component (describing, for example, the cryosphere and large bodies of surface water) has a somewhat smaller peak to peak amplitude of 2.4 ± 0.6 mm. Its phase implies that warming the oceans increases the ocean water loss rate. Additional much smaller terms include a steric feedback term and a fast eustatic term. The ENSO contributes a peak to peak variation of 5.5 ± 0.8 mm, predominantly through a direct effect on the MSL and significantly less so indirectly through variations in the radiative forcing.

1. Introduction

Several global climate variables appear to vary in sync with the solar cycle. These include average air temperatures and pressures [*Douglass and Clader*, 2002; *Shaviv*, 2005; *van Loon and Labitzke*, 2000], the sea surface temperature [*White et al.*, 1997], and the ocean heat content and sea level [*Shaviv*, 2008]. On longer time scales, there are additional correlations between solar activity and climate [e.g., *Neff et al.*, 2001; *Bond et al.*, 2001; *Wang et al.*, 2005]. These observed climate variations could be the result of a climate which is sensitive to *any* changes in the radiative forcing, including the small variations associated with the total solar irradiance. Alternatively, the large nonthermal solar activity variations could be amplified by a mechanism unrelated to the solar irradiance and inducing a large radiative forcing on the climate.

Measurements of the radiative forcing associated with variations in the ocean heat content (or the related sea level) can be used to quantify the solar radiative forcing over the solar cycle, of which the peak to peak value comes out to be about 1 W/m^2 [*Shaviv*, 2008]. Since this stands in stark contrast to the 0.17–0.24 W/m^2 variations associated with the direct solar forcing [*Fröhlich and Lean*, 1998, 2004; *Foukal et al.*, 2006; *Willson and Mordvinov*, 2003], it was concluded that solar activity should be affecting climate through a large radiative forcing and not through a very sensitive climate reacting to the small irradiance variations. Note that the forcing associated with the solar irradiance is $4(1-a)$ times smaller than the irradiance variations because of the surface to cross-section ratio of Earth and its finite albedo.

Two families of mechanisms were suggested to give this larger radiative forcing. The first includes hypersensitivity to UV [*Haigh*, 1994]. Although global circulation models show that the net effect on the surface temperature of this mechanism is at most to double the effect of the solar irradiance [*Lee and Smith*, 2003; *Haigh et al.*, 2005], there are significant uncertainties and room for a large contribution (see review of *Solanki et al.* [2013]). A second mechanism is sensitivity to the solar wind-modulated cosmic ray flux (CRF) that in turn modulates the Earth's cloud cover [*Ney*, 1959; *Svensmark and Friis-Christensen*, 1997; *Svensmark*, 1998]. Given independent correlations observed between CRF variations and climate on different time scales [e.g., *Shaviv*, 2002; *Svensmark et al.*, 2009], this mechanism involving clouds could potentially explain the amplified solar forcing or part of it. Interestingly, several experiments indicate that atmospheric ionization can increase the nucleation of condensation nuclei [*Svensmark et al.*, 2005; *Kirkby*, 2011] and help the growth to cloud condensation nuclei [*Svensmark et al.*, 2013]. Nevertheless, it should be noted that the solar/CRF/climate link

is still debated in the literature, partially because an exact chemical or physical mechanism is still missing and partially because some of the empirical evidence is disputed.

Our goal in the present analysis is to study the satellite altimetry data and elaborate on *Shaviv* [2008] who quantified the total radiative forcing associated with the solar cycle. There are several advantages in considering the additional data. First, the altimetry data provide an entirely independent data set to the tide gauges, sea surface temperature, and the ocean heat content considered by *Shaviv* [2008]. Moreover, its 1993–2013 time span only has a moderate overlap with the tide gauges data used by *Shaviv* [2008] that ended in 2000. Second, because of its higher signal-to-noise ratio and higher temporal resolution than that of the data sets considered by *Shaviv* [2008], the present altimetry data can offer information about phase and with it on the "calorimetric efficiency" of the oceans. This in turn will allow a better estimate of the radiative forcing associated with the solar cycle. Although this estimate cannot point to a particular mechanism, it can prove that a mechanism other than direct changes in the irradiance must be operating.

Since the El Niño–Southern Oscillation also appears to have a clear effect on the sea level [e.g., *Ngo-Duc*, 2005], we also include it in the model fit.

We begin in section 2 with a description of the data sets we use. We then continue in section 3 to construct an empirical model to fit the altimetry data. In section 4 we carry out a "zeroth-order" study of the solar forcing term. We show in the appendix that higher-order contributions are relatively small and only increase the uncertainty of the lowest-order analysis. In section 5, we use the results to derive the ocean's calorimetric efficiency over the solar cycle. We end with a discussion of the implications in section 6.

2. Data Sets Used

The altimetry data set used is derived from the TOPEX/Poseidon and Jason altimeter missions with the seasonal signals removed [*Nerem et al.*, 2010] (data electronically available at http://sealevel.colorado.edu/). The data we use have the inverse barometer and glacial isostatic adjustment corrections applied, and it covers the time period between mid-1993 to early 2013.

Several detailed discussions of the errors in the altimetry data exist [e.g., *Nerem and Mitchum*, 2001; *Fernandes et al.*, 2006; *Ablain et al.*, 2009; *Nerem et al.*, 2010]. They describe the many sources of errors, which as an example include orbital variations, dry and wet variations in the troposphere, solid Earth tide, or even variations in the ionosphere. These discussions often concentrate on the long-term "drifts" that will offset the estimated long-term sea level change rate. In the present analysis which aims at fingerprinting the solar and ENSO contributions, the linear term is removed. To estimate the error in a single 10 day data point, we note that a comparison between TOPEX/Poseidon and Jason-1 satellites, by *Leuliette et al.* [2004], gives a RMS residual difference of 1.6 mm. The error on annually smoothed data will be smaller. This RMS should therefore be considered as an upper limit.

For the El Niño–Southern Oscillation we use the NINO 3.4 index [*Trenberth*, 1997], which is based on the sea surface temperature in the middle of the Pacific (bounded by 120°W, 170°W, 5°S, and 5°N). Because this index is directly related to the oceanic temperature while the Southern Oscillation Index depends on atmospheric pressures, we expect the former to have less variations and to more directly reflect the ocean heat content.

Since we do not wish to limit ourselves to a particular mechanism for the solar forcing (such as hypersensitivity to UV or to cosmic rays), we will assume for simplicity that the forcing is harmonic, as we discuss below.

Since we are interested only in variations longer than the annual time scale, both data sets are "smoothed" by being passed through a 1 year moving average. They are depicted in Figure 1 after the smoothing filter has been applied. The 10 day altimetry data are then binned into months to have the same resolution as the NINO 3.4 index. Thus, the analysis is carried out on data having monthly resolution, but variations over the annual time scale or shorter are filtered out.

3. The Model Fit

We begin by fitting the satellite-based sea level data with an empirical model. We assume that the mean sea level (MSL) can be described by a long-term linear trend, a harmonic solar contribution, and a term reflecting the ENSO.

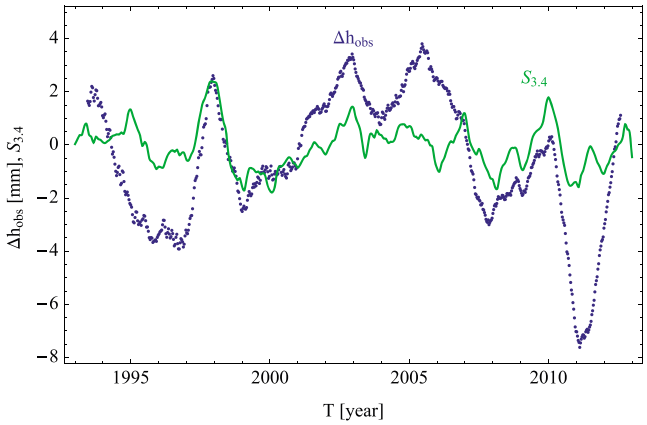

Figure 1. The two data sets used in the analysis, after having been filtered with a 1 year moving average. The first data set is the linearly detrended TOPEX/Poseidon and Jason altimetry data (Δh_{obs}), while the second is the NINO 3.4 Southern Oscillation Index ($S_{3.4}$). The former is binned into 1 month points before further used in the analysis, so as to have the same resolution as the $S_{3.4}$ data set.

We include a solar term in the model because a large solar component was observed in various oceanic data sets, including the ocean heat content, sea surface temperature, and the sea level [*Shaviv*, 2008]. Given the heat content variations, part of the solar component in the sea level should be due to thermal expansion, which is a steric component. Another component, however, could be eustatic (such as due to changes in the amount of surface water and ice). Since we a priori do not know the relative size of the different components, the phase of the solar contribution is unknown and it therefore should be left as a free parameter. The meaning of this phase will be discussed in the next section. Since the duration of the 23rd solar cycle has been 12.6 years, we force this period.

Since the expansion coefficient of water is temperature dependent, mixing water at different temperatures gives rise to a net MSL change. We therefore expect a MSL component that is directly related to the ENSO index we use. However, the Southern Oscillation can also impose a radiative forcing, for example, through a cloud cover that depends on the ocean temperatures (and therefore on the index). Since the heat content, and therefore thermal expansion, depends on the time integral of the radiative forcing, there could in principle be an additional sea level term that depends on the integral of the index we use, though as we shall see below, it is actually small compared with the zeroth-order component.

Last, we allow for a linear term because the MSL clearly has a long-term variation which arises from long-term climate change. For example, the melting of ice caps due to the net twentieth century warming gives rise to a monotonic sea level increase. Although interesting, this linear trend is not part of the present analysis.

Thus, we assume that the sea level can be approximated by

$$\Delta h(t) = h_0 + h_1(t - t_0) + a\cos\left(\frac{2\pi(t - t_0)}{P} + \phi\right) + b_0 S_{3.4}(t) + b_1 S_{I,3.4}(t). \quad (1)$$

Here h is the sea level height. $S_{3.4}$ is the ENSO (the NINO 3.4 index; see section 2), while $S_{I,3.4}$ is the time integral of $S_{3.4}$ with its average removed, that is,

$$S_{I,3.4}(t) \equiv \int_{t_0}^{t} S_{3.4}(t')\mathrm{d}t' - \left\langle \int_{t_0}^{t} S_{3.4}(t')\mathrm{d}t' \right\rangle, \quad (2)$$

where $\langle\rangle$ denotes a time average over the 1993 to 2013 interval. Because the average is removed, any t_0 can be used. We choose $t_0 = 2001.5$ years since it corresponds to the estimated time of solar maximum. Note that we will make below the distinction between ϕ, which is the phase lag relative to t_0, and θ, which is the phase lag relative to solar maximum. Given the definition of t_0, the angles coincide, but the uncertainty on θ will be larger as it will also include the uncertainty in the exact timing of the solar maximum. The free parameters that describe the linear trend in the altimetry data are h_0 and h_1, which can arise from any long-term process. The free parameters that describe the solar term are a and ϕ, while b_0 and b_1 are the free parameters that describe the ENSO contribution. Last, we take $P = 12.6$ years, which is the duration of the last solar cycle.

The fit is carried out by minimizing the χ^2 of the fit between the modeled $h(t)$ and the observed sea level. The parameters we find are given in Table 1. The model fit is depicted in Figure 2, while the separate solar and ENSO components are depicted in Figure 3.

An important aspect of the model fit is estimating the errors of the model parameters. One possible methodology would be to estimate the error by considering the statistical errors in the different data sets and their

Table 1. The Model Fit Parameters

Parameter	Value
h_0	15.4 ± 0.2 mm
h_1	3.29 ± 0.04 mm/yr
a	2.5 ± 0.4 mm
ϕ	$58° \pm 7$
b_0	1.2 ± 0.2 mm per $S_{3.4}$ unit
b_1	0.65 ± 0.3 mm/yr per $S_{3.4}$ unit

temporal correlation function and then propagate those errors to the fitted parameters. This is, however, tricky as it requires not only exact information on the measurement errors themselves but also information on the intrinsic climate variations. A second methodology is that of "bootstrapping," in which the data set itself is used to reliably carry out the error estimation [e.g., *Efron*, 1979; *Press et al.*, 1986; *Kunsch*, 1989]. This approach is often used when there is insufficient information about the underlying statistical processes or the nature of the measurement errors.

Specifically, we carry out the bootstrap error estimation by generating many degraded realizations having randomly chosen blocks of data replaced, as is detailed in *Kunsch* [1989]. Because the data sets are passed through a 1 year moving average, the random blocks are chosen to have random lengths between 1 and 3 years.

Although the bootstrap method is similar to the more familiar jackknifing, it has an important additional advantage. Because the data are relatively noisy, several local minima could potentially exist. However, since each realization of the bootstrap has significant degradation of the data (compared to the jackknife method which only removes one measurement at a time), we are more likely to sample a larger parameter phase space and obtain a more robust fit.

We find that the altimetry sea level data have two statistically significant components, one varies with the ENSO and one in sync with the Sun. There was no statistically significant improvement in the model fit when additional indices were used, such as the Pacific Decadal Oscillation and North Atlantic Oscillation.

We also find that the main ENSO contribution is the b_0 term, i.e., sea level variations which depend on the present state of the ENSO, and not its integral, which contributes only marginally. The situation is somewhat different for the solar contribution. Since solar maximum and resulting cosmic ray minimum occurred around 2001.5 ± 0.5, the value of ϕ implies that the phase lag relative to the solar maximum is $\theta = 58 \pm 16°$. As a consequence, the largest contribution is one which appears to be an integral of the solar radiative forcing, but it cannot explain all the sea level variation. The integral term would be expected from the thermal expansion of the oceans. However, in order to understand this better, we analyze below the phase in more detail.

Without the ENSO and solar components removed, the variance of the annually smoothed and linearly detrended sea level was 6.55 mm^2, while it is 1.88 mm^2 with the components removed. In other words, the model explains 71% of the variance. Similarly, a fit with only the solar component explains 51% of the observed variance, while a fit with only the ENSO component explains 23%. Note that the sum is a bit more than the total 71% explained by the model because of a small correlation between the solar and ENSO components over the interval considered.

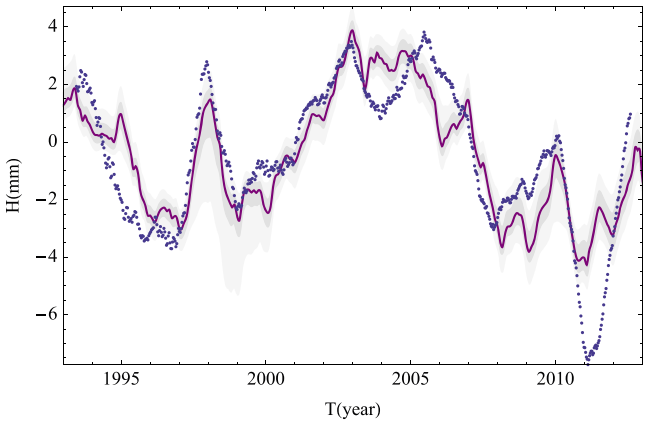

Figure 2. Sea level data and the model fit. The blue dots are the linearly detrended global sea level measured with satellite altimetry. The purple line is the model fit to the data which includes both a harmonic solar component and an ENSO contribution. The shaded regions denote the 1σ and 1% to 99% confidence regions. The fit explains 71% of the observed variance in the filtered detrended data.

4. Implications of the Solar Term

We have seen in the previous section that the sea level altimetry can be fitted with an empirical model that includes terms associated with the ENSO and the solar variations. The next step is to use the fitted parameters to derive constraints on the physical forcing terms. Here we shall

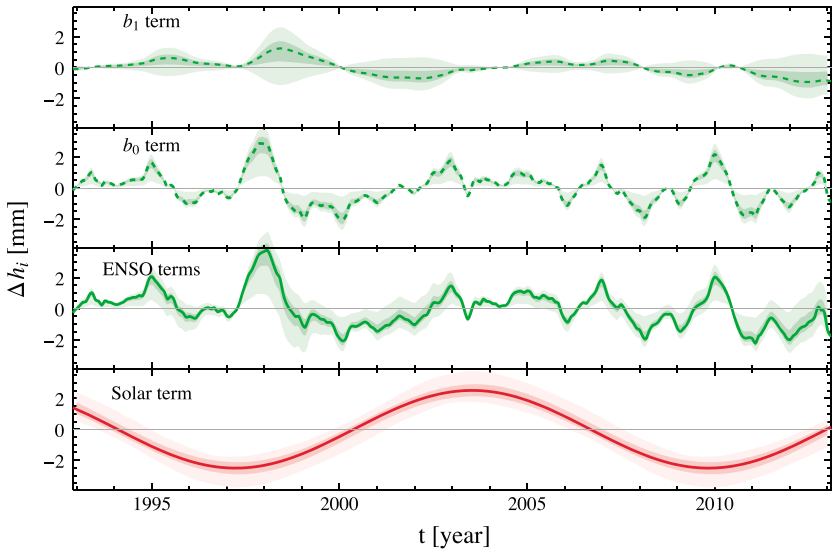

Figure 3. The ENSO and solar contributions in the model fit. The red and green curves respectively correspond to the solar and ENSO contributions in the model fit. Also depicted are the separate ENSO contributions, with the b_0 and b_1 terms depicted in thick dashed and thin dashed lines, respectively. The shaded regions denote the 1σ and 1% to 99% confidence regions.

do so for the solar forcing, which as we shall see has two primary components—a steric term associated with thermal expansion and a eustatic component, associated with water trapped in land reservoirs.

The above empirical fit assumed a harmonic solar forcing. Although it is only an approximation, it significantly simplifies the analysis. By describing the radiative forcing anomaly as a complex number: $\Delta F_{solar}(t) = \Delta F_{solar} \exp(-i\omega t)$, each component of the sea level can then be described with a complex amplitude. The phase will then describe a lag or lead relative to the solar forcing.

The simplest model is heuristically described in Figure 4. If we consider well-mixed oceans that only absorb the flux associated with the solar forcing, ΔF_{solar}, then the heat inside the oceans (per unit area) will simply be the integral of the forcing, $Q = \int \Delta F_{solar} dt$. In such a case, Q will lag ΔF_{solar} by 90°. The steric sea level component associated with the thermal expansion is proportional to Q, and it will therefore lag ΔF_{solar} by 90° as well.

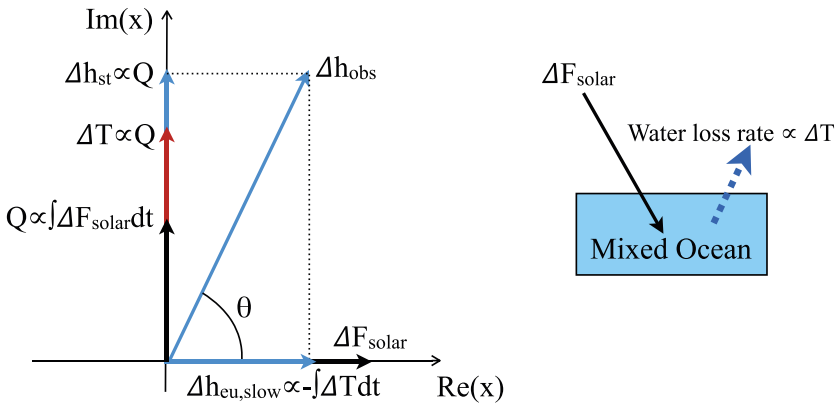

Figure 4. A heuristic phase diagram describing the expected solar contribution to sea level variations in a simple model which includes a well-mixed ocean, a sinusoidal solar forcing, and water loss rate that is proportional to the sea surface temperature. Here the steric component of the sea level, Δh_{st}, and the heat content Q to which it is proportional are both proportional to the integral of solar forcing ΔF_{solar}. They will therefore lag behind the forcing by 90°. Since the ocean is well mixed, the temperature change of the surface will be proportional to Q as well. However, if the water loss *rate* is proportional to the temperature, that is, that the derivative of the slow eustatic component $\Delta h_{eu,slow}$ is proportional to $-\Delta T$, then $\Delta h_{eu,slow}$ will have the same phase as the forcing. The sign, however, depends on whether a *warm* ocean causes a *greater water loss* and trapping in lakes and glaciers (which is the case plotted and empirically found), or the opposite.

The second important component affecting the sea level is the eustatic term associated with water loss from the oceans and which is trapped elsewhere, in slow to equilibrate reservoirs such as in the cryosphere or lakes. If the rate with which water leaves the oceans is proportional to the temperature anomaly $\Delta T(t)$, which itself is proportional to the heat content $Q(t)$, then this eustatic component $\Delta h_{\mathrm{eu,slow}}(t)$ will lag the heat content by another 90°. However, if the sign is such that an increase in the ocean temperature increases the *loss* rate, this eustatic term will actually be in phase with the solar forcing, as exemplified by the decrease in the net phase lag from 90°.

The phase found for the solar component is $\phi = 58 \pm 7°$, which corresponds to a peak in $\Delta h_{\mathrm{obs}}(t)$ in the year 2003.55 ± 0.25. On the other hand, solar maximum took place around 2001.5 ± 0.5. The uncertainty arises because the actual maximum depends on the component considered (e.g., sunspots, irradiance, or cosmic ray flux). Thus, the sea level lags the solar cycle by $\theta = 58 \pm 15°$.

Using the simple model described in Figure 4, we can therefore estimate the amplitude of each of the two sea level components to be

$$\Delta h_{\mathrm{st}}\big|_0 \approx \Delta h_{\mathrm{obs}} \sin\theta = 2.15 \pm 0.35 \text{ mm}, \tag{3}$$

$$\Delta h_{\mathrm{eu,slow}}\big|_0 \approx \Delta h_{\mathrm{obs}} \cos\theta = 1.25 \pm 0.2 \text{ mm}. \tag{4}$$

This simple model can be improved by adding higher-order contributions to the sea level change. This is carried out in the appendix, where it is found that with these additional terms, the amplitude estimates of the two sea level components are

$$\Delta h_{\mathrm{st}} = 2.2 \pm 0.4 \text{ mm}, \tag{5}$$

$$\Delta h_{\mathrm{eu,slow}} = 1.2 \pm 0.3 \text{ mm}. \tag{6}$$

Note that while they change the estimate by only a little, the additional terms do increase the uncertainty.

5. The Solar Radiative Forcing and Implied Calorimetric Efficiency

Using the estimate value of Δh_{st} and the expansion coefficient χ_{steric} relating heat content and sea level change, we can estimate the radiative forcing to be

$$\Delta F_{\mathrm{solar}} = \frac{\Delta h_{\mathrm{st}}}{\chi_{\mathrm{steric}}} \frac{2\pi}{P} = 0.66 \pm 0.17 \text{ W/m}^2. \tag{7}$$

This is the amplitude of the forcing. The peak to peak variations will be twice larger and equal to 1.33 ± 0.35 W/m^2.

We can also estimate the calorimetric efficiency, ϵ, which is the fraction of the sea level change actually associated with thermal expansion. It is

$$\epsilon = \frac{\Delta h_{\mathrm{st}}}{\Delta h_{\mathrm{obs}}} \approx 0.9. \tag{8}$$

6. Discussion

The main result of the analysis presented is that the Sun and the ENSO are by far the dominant drivers of sea level change on the annual to decade time scale. If the linear trend is removed, the two drivers explain more than 70% of the variance of the annually smoothed (with a 1 year moving average) and linearly detrended data. The two contributions should come with no surprise as they were previously reported.

A large ENSO component was already found to be present in the satellite altimetry data [e.g., *Ngo-Duc*, 2005]. Our additional contribution here was to demonstrate that it is primarily through a term proportional to the ENSO index. On the other hand, the term proportional to the integral of the ENSO index is small. This implies that there is relatively little radiative forcing associated with the ENSO. Such a direct ENSO sea level relation can be naturally explained if the ENSO is primarily an oscillation that mixes water in the Pacific basin, which changes the sea level due to the nonlinear temperature dependence of the expansion coefficient.

Likewise, a significant solar contribution to the MSL was also previously reported but in the tide gauge records [*Shaviv*, 2008]. However, since the data set used in the present analysis is that of satellite altimetry and it has only a small overlap with the tide gauge records, the result using the present data set is an independent corroboration of the previous result, though with higher-quality data—having a better signal-to-noise ratio and a higher temporal resolution than the tide gauge data (though with a shorter span). This allows carrying out a detailed phase analysis that cannot be achieved with the tide gauges.

Furthermore, the more detailed phase analysis allowed us to differentiate between the two major contributions to the MSL on the decadal time scale. One is the solar forcing, while the second is that of slow eustatic variations in the sea level, from water trapped in surface reservoirs. The solar forcing could be quantified, with the peak to peak variations found to be 1.33 ± 0.35 W/m^2. The eustatic solar term was found to be about half as large as the steric solar term. Interestingly, its sign implies that a higher ocean temperature gives rise to a higher rate of water leaving the ocean basins and getting trapped on land, thus lowering the sea level. This is opposite from the long-term expectation, where warmer oceans should cause the melting of the cryosphere and a rise in sea level.

The large forcing associated with the solar cycle is consistent with previous calorimetric determination of the solar radiative forcing [*Shaviv*, 2008] and with the radiative forcing obtained when minimizing the residuals between the simulated twentieth century climate change and the actual observations [*Ziskin and Shaviv*, 2011]. It also corroborates previous claims that a mechanism must be operating to amplify the solar activity. Just the variations in the total solar irradiance correspond to a radiative forcing of 0.17–0.24 W/m^2, but the amount of heat entering the ocean over the solar cycle appears to be much larger. The next step from here would be to take a full-fledged global circulation model and study whether some climate mechanism could mimic such a large flux, while in parallel the community should also consider mechanisms that could actually give rise to a large radiative flux over the solar cycle.

Appendix A: A More Detailed Analysis of the Model Fit

This simple model can be improved as is described in Figure A1. First, instead of assuming just a mixed layer, one can add the deep ocean which warms (or cools) through diffusion beneath the mixed layer, with some diffusion coefficient κ. The ocean can also interact with the climate system above it through a feedback that depends on the temperature of the ocean surface (i.e., the mixed layer), $\Delta F_{\mathrm{fb}}(t) = -\lambda \Delta T(t)$. An analytical solution to this problem can be found in *Shaviv* [2008]. The main property of this solution relevant for the present analysis is that the mixed layer temperature $\Delta T(t)$ does not lag the radiative forcing by 90° but by a smaller angle. For a wide range of ocean diffusivities and feedbacks λ, this angle α was found to range between 55° and 70°.

Another modification is to consider that there are two types of eustatic contributions to the sea level. The large one, $\Delta h_{\mathrm{eu,slow}}$, is the term describing water being trapped in "slow" reservoirs, which was considered in the main part of the text. The rate of change of this sea level term will depend on the rate of change of the temperature, thus leading the solar forcing by $90° + \alpha$. Again, we assume here that warmer oceans increase the water loss rate. Thus, the actual sign will be negative, and the term will actually appear to be leading the solar forcing by $90° - \alpha$.

A second term, however, is a fast eustatic component, $\Delta h_{\mathrm{eu,fast}}$, which describes water present in reservoirs that equilibrate on time scales much shorter than the 11 year solar cycle, such as water in the atmosphere and on the surface. This term will be proportional to the mixed layer temperature anomaly, with opposite sign (as warmer oceans imply that more water is present in the atmosphere and on land), and it will therefore lag the solar forcing by $180° + \alpha$ (or equivalently lead by $\alpha - 180°$).

Adding these terms together gives

$$\begin{aligned} \Delta h_{\mathrm{obs}} \cos\theta &= \left(\Delta h_{\mathrm{eu,slow}} + \Delta h_{\mathrm{steric,fb}}\right) \sin\alpha - \Delta h_{\mathrm{eu,fast}} \cos\alpha\,, \\ \Delta h_{\mathrm{obs}} \sin\theta &= \Delta h_{\mathrm{st}} - \left(\Delta h_{\mathrm{eu,slow}} + \Delta h_{\mathrm{steric,fb}}\right) \cos\alpha - \Delta h_{\mathrm{eu,fast}} \sin\alpha, \end{aligned} \tag{A1}$$

where Δh_{st} is the steric term expected with no feedbacks or additional effects.

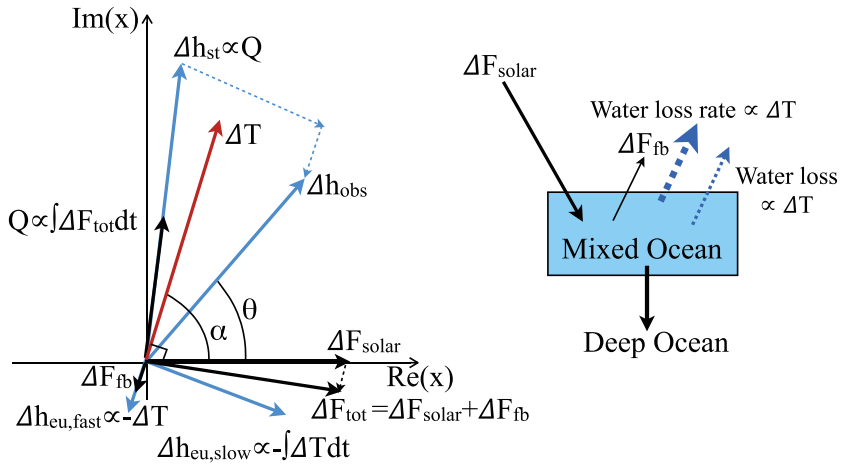

Figure A1. A heuristic phase diagram describing the expected solar contribution to sea level variations in a more general model described in the appendix, which includes additional components to those described in the Figure 4. First, if we include the interaction of the mixed layer with the deep ocean through diffusion, the temperature of the mixed layer is no longer lagging by 90° but by less. For the observed range of ocean diffusivities and a conservative range of ocean temperature sensitivities, the phase α is found to be 55 to 70° instead [*Shaviv*, 2008]. Next, as the ocean warms, it will lose some of its heat through feedback, with $\Delta F_{fb} = -\lambda \Delta T$. The heat content will therefore be the integral of the total flux $\Delta F_{tot} = \Delta F_{solar} + \Delta F_{fb}$. Since the feedback tends to cool the ocean as it heats up, Q will now lag the forcing by less than 90°. We can also describe the water loss from the oceans more generally. In addition to the slow component for which the water loss rate is proportional to the temperature (through trapping of water in slow to respond reservoirs), there could also be a fast component whereby increasing the water temperature traps water in fast components, such as the atmosphere or rivers. Since there will be more evaporation for a higher temperature, this latter term, $\Delta h_{eu,fast}$, will be in the opposite phase as ΔT.

Clearly, if we only measure two numbers, Δh_{obs} and θ, we cannot find the values of four unknowns: $\Delta h_{eu,slow}$, $\Delta h_{eu,fast}$, Δh_{st}, and Δh_{fb}. Thus, in what follows we will place a theoretical limit on both $\Delta h_{eu,fast}$ and Δh_{fb} and show that they are relatively small. This will allow us to derive Δh_{st} and $\Delta h_{eu,slow}$:

$$\Delta h_{st} = \Delta h_{obs}\,[1 + \cot(\alpha)]\cos(\theta) + \frac{\Delta h_{eu,fast}}{\sin(\alpha)}, \tag{A2}$$

$$\Delta h_{eu,slow} = -\Delta h_{fb} + \Delta h_{eu,fast}\cot(\alpha) + \frac{\Delta h_{obs}\cos\theta}{\sin(\alpha)}. \tag{A3}$$

We will then use the first relation to derive the size of the forcing ΔF_{solar}.

Estimating $\Delta h_{eu,fast}$. As the oceans absorb heat and increase their surface temperature, the atmosphere which is in rough equilibrium with the oceans will contain more water vapor and the amount of water circulating over land will increase as well. If the residency time of water in the "fast" reservoirs is constant, the amount of water will increase in proportion to the absolute increase in the water vapor. Over the solar cycle, the peak to peak ocean surface temperature changes by about 0.08°C [e.g., *Shaviv*, 2005, and references therein]. From the Clausius-Clapeyron equation, the relative change in the absolute humidity variations due to the observed oceanic temperature change is $f_{fs} \approx 0.5\%$. This assumes that the atmosphere keeps a constant relative humidity.

Furthermore, the water reservoirs that equilibrate on time scales shorter than a year include the atmosphere, soil moisture, rivers, and biological water. According to *Shiklomanov* [1993], they add up to $V_{fs} \approx 165$ km^3. Given the relative change in the absolute humidity over the solar cycle, the sea level should change by $\Delta h_{eu,fast} \approx \Delta V_{fs}/2A_{oceans}$ where ΔV_{fs} is the net volume change due to the fast eustatic variations over the solar cycle while A_{ocean} is the ocean surface area. The factor 2 arises since we used the peak to peak temperature variations, though we work with harmonic amplitudes. We therefore obtain $\Delta h_{eu,fast} \approx f_{fs} V_{fs}/2A_{oceans} \approx 0.25$ mm. The sign is such that by increasing oceanic temperature, more water circulates outside the oceans and the sea level is lower. From comparison to Figure A1 and equation (3), it is evident that this component is small but not entirely negligible.

Estimating Δh_{fb}. To estimate Δh_{fb}, we again note that the peak to peak temperature variations are about 0.08°C. This temperature variation can be translated into the feedback forcing and then to a sea level change.

For the former relation, we note that the feedback is related to the ocean temperature sensitivity—any change in the radiative forcing gives rise to a changed temperature required to balance the radiative imbalance. A sensitive climate will require the oceans to have a large change in the temperature to do so. A very conservative range for the ocean temperature sensitivity would correspond to a temperature increase of $\Delta T_{\times 2} = 1 - 5$°C following a CO_2 doubling. If the latter corresponds to a radiative forcing of $\Delta F_{\times 2} \approx 3.7$ W/m^2 [*Myhre et al.*, 1998], then the feedback parameter is $\lambda = \Delta F_{\times 2}/\Delta T_{\times 2} \approx (0.75–4)$ (W/m^2)/°C.

The 0.08° peak to peak temperature variations will therefore correspond to a forcing term of $\Delta F_{fb} = 0.19 \pm 0.13$ W/m^2.

In order to translate the radiative forcing into a sea level change, we require the thermal expansion coefficient of water and note that it is temperature dependent. One therefore requires the average temperature of the oceans and the assumption that the oceans heat uniformly. The ratio χ between the ocean heat content variations and the sea level change rate can be derived in two ways [*Shaviv*, 2008]. First, if one averages the temperature of the mixed layer, one finds that the temperature-dependent *heat content* (and not thermal) expansion coefficient is $\chi_{steric} = 1.35$ (mm/yr)/(W/m^2). Second, one can compare measured temperature variations to measured ocean heat content variations on somewhat longer time scales [*Levitus and Boyer*, 1994; *Ishii et al.*, 2006] and obtain $\chi_{steric} = 1.95 \pm 0.2$ (mm/yr)/(W/m^2). We will take the average as our nominal value but use the difference as an estimate for the error; that is, we take

$$\chi_{steric} = 1.65 \pm 0.3 \frac{\text{mm/yr}}{\text{W/m}^2}. \tag{A4}$$

Using the above feedback forcing, we obtain

$$\Delta h_{fb} = \frac{\Delta \chi F_{fb}}{2} \frac{P}{2\pi} = 0.3 \pm 0.2 \text{ mm}. \tag{A5}$$

Clearly, the feedback term is not expected to be important.

Finally, with estimates for $\Delta h_{eu,fast}$ and Δh_{fb}, which are both relatively small, we can estimate Δh_{st} and $\Delta h_{eu,slow}$ using equation (A2). We find

$$\Delta h_{st} = 2.2 \pm 0.4 \text{ mm} \tag{A6}$$

$$\Delta h_{eu,slow} = 1.2 \pm 0.3 \text{ mm}. \tag{A7}$$

Acknowledgments
All data sets used have been previously published by others, and they are readily available in references appearing in section 2. This research project was supported by the I-CORE Program of the Planning and Budgeting Committee and the Israel Science Foundation (center 1829/12). N.J.S. also thanks the IBM Einstein Fellowship support by the IAS.

Yuming Wang thanks the reviewers for their assistance in evaluating this paper.

References

Ablain, M., A. Cazenave, G. Valladeau, and S. Guinehut (2009), A new assessment of the error budget of global mean sea level rate estimated by satellite altimetry over 1993–2008, *Ocean Sci.*, *5*(2), 193–201, doi:10.5194/os-5-193-2009.

Bond, G., B. Kromer, J. Beer, R. Muscheler, M. N. Evans, W. Showers, S. Hoffmann, R. Lotti-Bond, I. Hajdas, and G. Bonani (2001), Persistent Solar influence on North Atlantic climate during the Holocene, *Science*, *294*, 2130–2136.

Douglass, D. H., and B. D. Clader (2002), Climate sensitivity of the Earth to solar irradiance, *Geophys. Res. Lett.*, *29* (16), 33-1–33-4, doi:10.1029/2002GL015345.

Efron, B. (1979), Bootstrap methods: Another look at the jackknife, *Ann. Stat.*, *7*(1), 1–26, doi:10.1214/aos/1176344552.

Fernandes, M. J., S. Barbosa, and C. Làzaro (2006), Impact of altimeter data processing on sea level studies, *Sensors*, *6* (3), 131–163, doi:10.3390/s6030131.

Foukal, P., C. Fröhlich, H. Spruit, and T. M. L. Wigley (2006), Variations in solar luminosity and their effect on the Earth's climate, *Nature*, *443*, 161–166, doi:10.1038/nature05072.

Fröhlich, C., and J. Lean (1998), The Sun's total irradiance: Cycles, trends and related climate change uncertainties since 1976, *Geophys. Res. Lett.*, *25*, 4377–4380, doi:10.1029/1998GL900157.

Fröhlich, C., and J. Lean (2004), Solar radiative output and its variability: Evidence and mechanisms, *Astron. Astrophys. Rev.*, *12*(4), 273–320.

Haigh, J. D. (1994), The role of stratospheric ozone in modulating the solar radiative forcing of climate, *Nature*, *370*, 544–546, doi:10.1038/370544a0.

Haigh, J. D., M. Blackburn, and R. Day (2005), The response of tropospheric circulation to perturbations in lower-stratospheric temperature, *J. Clim.*, *18*, 3672–3685, doi:10.1175/JCLI3472.1.

Ishii, M., M. Kimoto, K. Sakamoto, and S. Iwasaki (2006), Steric sea level changes estimated from historical ocean subsurface temperature and salinity analyses, *J. Ocean.*, *62*, 155–170.

Kirkby, J. E. A. (2011), Role of sulphuric acid, ammonia and galactic cosmic rays in atmospheric aerosol nucleation, *Nature*, *476*, 429–433, doi:10.1038/nature10343.

Kunsch, H. R. (1989), The jackknife and the bootstrap for general stationary observations, *Ann. Stat.*, *17* (3), 1217–1241, doi:10.1214/aos/1176347265.

Lee, H., and A. K. Smith (2003), Simulation of the combined effects of solar cycle, quasi-biennial oscillation, and volcanic forcing on stratospheric ozone changes in recent decades, *J. Geophys. Res.*, *108*(D2), 4049, doi:10.1029/2001JD001503.

Leuliette, E. W., R. S. Nerem, and G. T. Mitchum (2004), Calibration of TOPEX/Poseidon and Jason altimeter data to construct a continuous record of mean sea level change, *Mar. Geod.*, *27*(1–2), 79–94, doi:10.1080/01490410490465193.

Levitus, S., and T. Boyer (1994), World Ocean Atlas 1994. Volume 4. Temperature, *Tech. rep., PB–95-270112/XAB; NESDIS-4*, Natl. Environ. Satell., Data, and Inf. Serv., Washington, D. C. [Available at http://iridl.ldeo.columbia.edu/SOURCES/.LEVITUS94/.]

Myhre, G., E. J. Highwood, K. P. Shine, and F. Stordal (1998), New estimates of radiative forcing due to well mixed greenhouse gases, *Geophys. Res. Lett.*, *25*(14), 2715–2718.

Neff, U., S. J. Burns, A. Mangini, M. Mudelsee, D. Fleitmann, and A. Matter (2001), Strong coherence between solar variability and the monsoon in Oman between 9 and 6 kyr ago, *Nature*, *411*, 290–293.

Nerem, R., and G. Mitchum (2001), Chapter 8 sea level change, in *Satellite Altimetry and Earth Sciences: A Handbook of Techniques and Applications*, edited by L. Fu, and A. Cazenave, pp. 329–349, Elsevier, Amsterdam, doi:10.1016/s0074-6142(01)80153-4.

Nerem, R., D. Chambers, C. Choe, and G. Mitchum (2010), Estimating mean sea level change from the TOPEX and Jason altimeter missions, *Mar. Geod.*, *33*(S1), 435–446.

Ney, E. P. (1959), Cosmic radiation and weather, *Nature*, *183*, 451.

Ngo-Duc, T. (2005), Contribution of continental water to sea level variations during the 1997–1998 El Niño–Southern Oscillation event: Comparison between atmospheric model intercomparison project simulations and TOPEX/Poseidon satellite data, *J. Geophys. Res.*, *110*, D09103, doi:10.1029/2004JD004940.

Press, W. H., B. P. Flannery, and S. A. Teukolsky (1986), *Numerical Recipes: The Art of Scientific Computing*, Cambridge, Univ. Press, Cambridge, U. K.

Shaviv, N. J. (2002), Cosmic ray diffusion from the galactic spiral arms, iron meteorites, and a possible climatic connection, *Phys. Rev. Lett.*, *89*(5), 051102.

Shaviv, N. J. (2005), On climate response to changes in the cosmic ray flux and radiative budget, *J. Geophys. Res.*, *110*, A08105, doi:10.1029/2004JA010866.

Shaviv, N. J. (2008), Using the oceans as a calorimeter to quantify the solar radiative forcing, *J. Geophys. Res.*, *113*, A11101, doi:10.1029/2007JA012989.

Shiklomanov, I. (1993), World fresh water resources, in *Water in Crisis: A Guide to the World's Fresh Water Resources*, edited by P. H. Gleick, pp. 13–24, Oxford Univ. Press, New York.

Solanki, S. K., N. A. Krivova, and J. D. Haigh (2013), Solar irradiance variability and climate, *Annu. Rev. Astron. Astrophys.*, *51*(1), 311–351, doi:10.1146/annurev-astro-082812-141007.

Svensmark, H. (1998), Influence of cosmic rays on Earth's climate, *Phys. Rev. Lett.*, *81*, 5027–5030.

Svensmark, H., and E. Friis-Christensen (1997), Variation of cosmic ray flux and global cloud coverage—A missing link in solar-climate relationships, *J. Atmos. Sol. Terr. Phys.*, *59*(11), 1225–1232.

Svensmark, H., J. P. Pedersen, N. Marsh, M. B. Enghoff, and U. Uggerhoj (2005), New ion-nucleation mechanism relevant for the Earth's atmosphere: Experimental results, *Eos Trans. AGU*, *86*(52), Fall Meet. Suppl., Abstract A52B-06.

Svensmark, H., T. Bondo, and J. Svensmark (2009), Cosmic ray decreases affect atmospheric aerosols and clouds, *Geophys. Res. Lett.*, *36*, L15101, doi:10.1029/2009GL038429.

Svensmark, H., M. B. Enghoff, and J. O. P. Pedersen (2013), Response of cloud condensation nuclei (>50 nm) to changes in ion-nucleation, *Phys. Lett. A*, *377*, 2343–2347, doi:10.1016/j.physleta.2013.07.004.

Trenberth, K. E. (1997), The definition of El Niño, *Bull. Am. Meteorol. Soc.*, *78*(12), 2771–2777.

van Loon, H., and K. Labitzke (2000), The influence of the 11-year Solar cycle on the stratosphere below 30 km: A Review, *Space Sci. Rev.*, *94*, 259–278.

Wang, Y., et al. (2005), The Holocene Asian monsoon: Links to solar changes and North Atlantic climate, *Science*, *308*(5723), 854–857.

White, W. B., J. Lean, D. R. Cayan, and M. D. Dettinger (1997), Response of global upper ocean temperature to changing solar irradiance, *J. Geophys. Res.*, *102*, 3255–3266, doi:10.1029/96JC03549.

Willson, R. C., and A. V. Mordvinov (2003), Secular total solar irradiance trend during solar cycles 21–23, *Geophys. Res. Lett.*, *30*(5), 1199, doi:10.1029/2002GL016038.

Ziskin, S., and N. Shaviv (2011), Quantifying the role of solar radiative forcing over the 20th century, *Adv. Space Res.*, *50*, 762–776.